J Plant Dis Prot (2016) 123:267–271
DOI 10.1007/s41348-016-0042-z

SHORT COMMUNICATION

Morphological and molecular identification of *Neopestalotiopsis mesopotamica* causing tomato fruit rot

Najmeh Ayoubi[1] · **Sina Soleimani Pari**[2]

Received: 23 August 2016 / Accepted: 27 August 2016 / Published online: 15 September 2016

Abstract Severe fruit rot symptoms were observed on tomato crop (*Lycopersicon esculentum*) located in Hamedan province of Iran, in spring 2014. Affected fruits showed gray to dark spot that expanded rapidly. A fungus was consistently isolated from infected fruits. On the basis of morphological and cultural characteristics, as well as the sequences of the internal transcribed spacer region, β-tubulin and *tef1* taxonomic markers, the fungus was identified as *Neopestalotiopsis mesopotamica*. This is the first report of tomato fruit rot caused by *N. mesopotamica* in Iran and the world.

Keywords ITS · β-Tubulin · *Lycopersicon esculentum* · Taxonomy · *tef1*

Tomatoes (*Lycopersicon esculentum* Mill) belonging to the Solanaceae family are widely consumed either fresh or processed. Tomatoes are known as health-stimulating fruit because of the antioxidant properties of its main compounds, and so they are widely planted and used for local consumption in the world as well as in Iran. During the spring of 2015, numerous gray spots with irregular shapes, 5–8 mm in diameter, were observed on tomato fruits. The spots expanded into 6–10 mm in diameter over the time and became gray to black circles (Fig. 1c). More than 35 % of tomato crops were severely damaged by the disease in several fields. In severe cases, lesions coalesced to form large necrotic areas on the infected fruits.

Small tissue pieces from the edges of fruits lesions were disinfected in 1 % (w/v) sodium hypochlorite for 2 min, rinsed thrice in sterile distilled water, plated onto potato dextrose agar (PDA) and incubated at 25 °C with 12-h dark and light cycle for 5 days. A hyphal tip taken from the advancing edge of a 5-day-old actively growing culture was transferred to PDA. According to the colony and conidia morphology (number of cells and appendages), the isolates were initially identified as *Pestalotiopsis* sp. [4].

Recently, Maharachchikumbura et al. [9] based on combined morphological and molecular data of 91 *Pestalotiopsis* isolates segregated two novel genera, namely *Neopestalotiopsis* and *Pseudopestalotiopsis*. According to Maharachchikumbura et al. [9], the characterization of our *Pestalotiopsis* isolates was carried out based on both morphological and molecular analyses. For further studies, the morphological features of each colony, such as color, growth rate, texture and mycelial form, were noted and recorded. Sporulation was induced by placing sterilized carnation leaves on the surface of PDA medium with growing mycelia [6]. Colonies on PDA reached 7 cm diameter after 6 days at 25 °C in the dark, with crenate edge, whitish, with aerial mycelium on surface. Black and globular pycnidial conidiomata appeared after 10 days at 25 °C in dark (Fig. 1a, b). For micro-morphological observations, microscopic mounts were made in lactic acid and a drop of alcohol was added to remove air bubbles and excess conidia. The microscopic characterization of conidiomata and conidia was performed, using an Olympus BX50 light microscope. Fifty conidia from each isolate were chosen randomly to measure length and width and other morphological characteristics. Conidia 20–26 µm × 7.0–9.7 µm (average: 23 × 8.2 µm), fusiform, straight to slightly curved, 4-septate; basal cell conical and

✉ Sina Soleimani Pari
sina@alumni.ubc.ca

[1] Department of Plant Protection, College of Agriculture, Bu-Ali Sina University, Hamedan, Islamic Republic of Iran

[2] Department of Biology, University of British Columbia, 4200-6270 University Blvd, Vancouver, BC V6T 1Z4, Canada

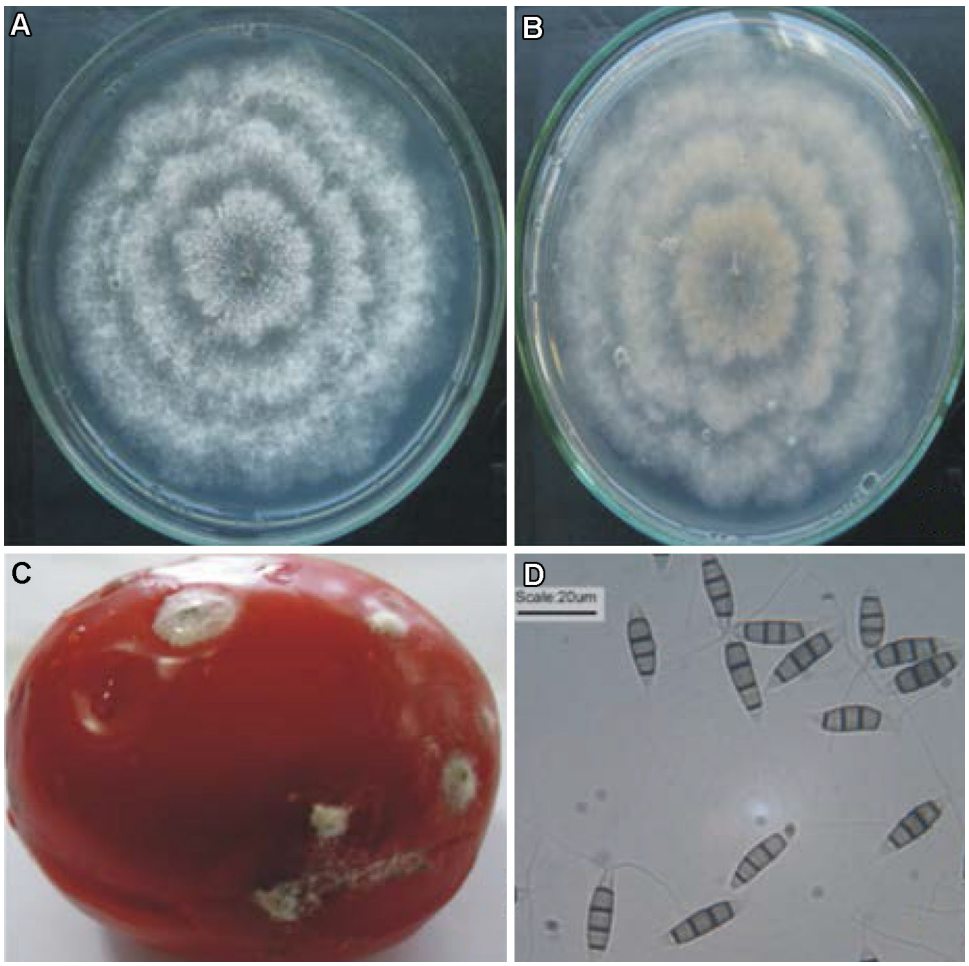

Fig. 1 *Neopestalotiopsis mesopotamica*; colony on PDA (**a** from above, **b** from below); symptoms on tomato fruit (**c**). Conidia, with versicolorous median cells, on PDA (**d**); *scale bars* 20 μm

hyaline 2.3–5.2 μm long (avg. 3.6 μm); three median cells 12–19.5 μm long (avg. 17 μm), dark brown, verruculose, septa and periclinal walls darker than the rest of the cell, versicolored, second cell from base pale brown, 3–6.8 μm (avg. 4.5 μm); third cell darker brown, 3.2–6.8 μm (avg. 4.8 μm); fourth cell darker, 3.4–7 μm (avg. 4.9 μm); apical cell 2.5–6.0 μm long (avg. 4.2 μm), hyaline, conical to cylindrical (Fig. 1d). The single basal appendage of conidia was 2.7–7.6 μm (avg. 5.2 μm) in length. The apical cell was hyaline and filiform, with 2–4 (mainly 3) apical appendages, 25.5–36.5 μm long (avg. 29.5 μm) (Fig. 1d). Photographs were taken using an Olympus digital camera installed on a BX50 Olympus light microscope.

Genomic DNA was extracted from fungal mycelia as described by Doyle and Doyle [2]. Since the ITS sequence data have relatively poor species resolution for the genus *Pestalotiopsis* [6], we have also used *tef1* and β-tubulin as additional barcode markers for their better species resolution and PCR success rate, within the *Pestalotiopsis* species. Partial DNA of a representative fungal isolate P816 (CBS137769) was amplified using ITS1 and ITS4 primer pairs for ITS regions, BT2A and BT2B for β-tubulin gene region, EF1-526F and EF1-1567R for *tef1* (Table 1). The amplified sequences were analyzed with other *Pestalotiopsis* group sequences listed in Table 2. The sequences of the three amplified products (ITS, BT2B and *tef1*) were then deposited in the GenBank database and assigned accession numbers KM074049 (ITS), KM074059 (BT2B) and KM074050 (*tef1*). The single locus dataset and combined multi-locus dataset of three gene regions were aligned using CLUSTALX2. Phylogenetic analyses of the sequence data consisted of Bayesian inference (BI) and maximum parsimony (MP) analyses of the combined aligned dataset. Suitable models for the Bayesian analysis were first selected using models of nucleotide substitution for each gene, as determined using MrModeltest v. 2.2 [10]. The Bayesian analyses (MrBayes v. 3.2.1; [11]) were done using random trees for 1,000,000 generations. The MP analysis was performed with phylogenetic analysis using parsimony (PAUP) v. 4.0b10 [12]. Trees were inferred by using the heuristic search option with TBR branch swapping and 1000 random sequence additions. The resulting trees were printed with Tree viewX.

Table 1 Primers used in this study

Primer name		Sequences
ITS (ITS1, 5.8S and ITS2) regions	ITS 1	5′-TCC GTA GGT GAA CCT GCG G-3′
	ITS4	5′-TCC TCC GCT TAT TGA TAT GC-3′
β-Tubulin gene region	BT2A	5′-GGT AAC CAA ATC GGT GCT GCT TTC-3′
	BT2B	5′-ACC CTC AGT GTA GTG ACC CTT GGC-3′
Partial translation elongation factor 1-alpha (*tef1*)	EF1-526F	5′-GTC GTY GTY ATY GGH CAY GT-3′
	EF1-1567R	5′-ACH GTR CCR ATA CCA CCR ATC TT-3′

Table 2 List of isolates used to draw the phylogenetic tree

Taxa	Isolates	GenBank accession number		
		ITS	β-tubulin	*tef1*
N. mesopotamica	CBS 299.74	KM199361	KM199435	KM199541
N. mesopotamica	P816 (CBS137769)	KM074049	KM074059	KM074050
N. clavispora (G.F. Atk.) Steyaert	MFLUCC 12-0280	JX398978	JX399013	JX399044
N. clavispora	MFLUCC 12-0281	JX398979	JX399014	JX399045
P. coffeeae-arabica	HGUP4015	KF412647	KF412641	KF412644
P. coffeeae-arabica	HGUP4019	KF412649	KF412643	KF412646
N. ellipsospora Maharachch. & K.D. Hyde	MFLUCC 12-0283	JX399016	JX399016	JX399047
N. ellipsospora	MFLUCC 12-0284	JX399015	JX399015	JX399046
N. foedans (Sacc. & Ellis) Steyaert	CGMCC 3.9123	JX398987	JX399022	JX399053
N. foedans	CGMCC 3.9202	JX398988	JX399023	JX399054
N. magna Maharachch. & K.D. Hyde	MFLUCC 12-652	KF582795	KF582793	KF582791
N. samarangensis Maharachch. & K.D. Hyde	MFLUCC 12-0233	JQ968609	JQ968610	JQ968611
N. saprophyte Maharachch. & K.D. Hyde	MFLUCC 12-0282	JX398982	JX399017	JX399048
N. steyaertii	IMI 192475	KF582796	KF582794	KF582792
N. umberspora Maharachch. & K.D. Hyde	MFLUCC 12-0285	JX398984	JX399019	JX399050
Seiridium sp.	SD096	JQ683725	JQ683709	JQ683741

The 50% consensus trees and posterior probabilities were calculated from the trees left after discarding trees (the first 25 % of generations) (Fig. 2). The parsimony analysis indicated that 1700 characteristics were constant, 267 variable characteristics parsimony-uninformative and 70 characteristics parsimony-informative. After a heuristic search using PAUP, six parsimonious trees were obtained (tree length = 420 steps, CI = 0.895, RI = 0.672, RC = 0.601, HI = 0.105). The Bayesian analysis resulted in a tree with the same topology and clades as the ML and MP trees.

Based on these molecular and morphological criteria, the fungus was identified as *Neopestalotiopsis mesopotamica* according to those original cultural and morphological characteristics described by Maharachchikumbura et al. [9]. The cultural and micro-morphological characteristics also were similar to those of *N. mesopotamica*, since they have been characterized by versicolorous median cells and 2–4 apical appendages (mainly 3) (Fig. 1d). In addition each analysis revealed high support (pp = 0.99, bs = 85 %) for our *N. mesopotamica* isolate P816 (CBS137769)/*N. mesopotamica* CBS 299.74 clade, revealing a close relationship between these species (Fig. 2).

Pathogenicity tests were performed on ten tomato plants bearing four tomato fruits. Conidial suspension containing 1×10^5 CFU/ml of our isolate (P816) was sprayed on each tomato plant. Infected tomato crops were incubated in a growth chamber at 90 % relative humidity and a 12-h photoperiod. Koch's postulates were verified by isolating the *N. mesopotamica* fungus consistently from symptomatic fruits after 2 weeks. Non-inoculated controls sprayed with sterile distilled water, remained healthy. Representative culture (P816) from original isolation of

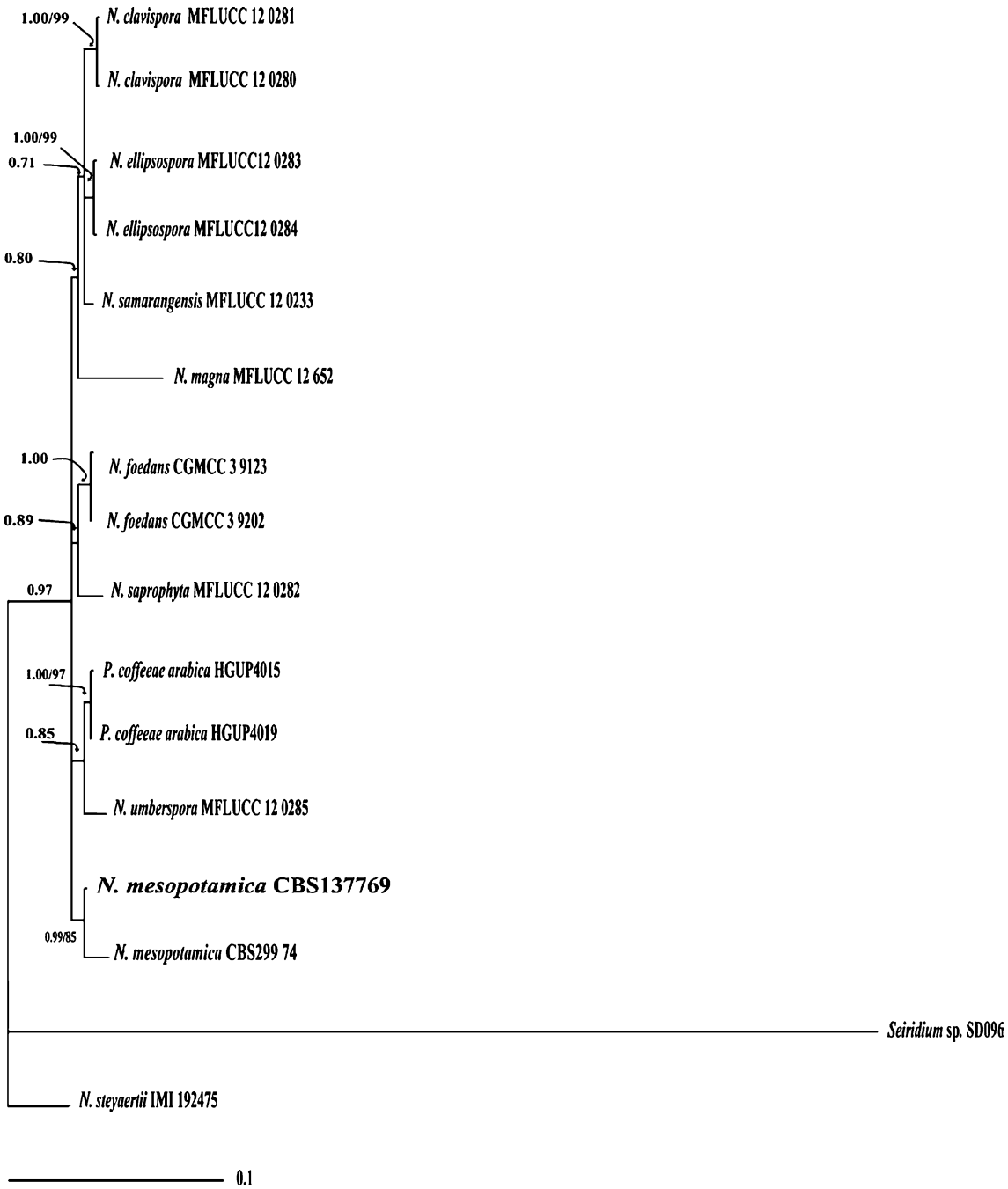

Fig. 2 Phylogenetic summary of relationships among some *Neopestalotiopsis* species given from NCBI and CBS137769 isolate resulting from Bayesian inference (BI) and maximum parsimony (MP) analyses of a combined ITS + TUB + TEF data matrix. This phylogram is the resulting 50 % majority rule consensus tree from the BI analysis with corresponding posterior probabilities (PP) and maximum parsimony bootstrap supports (MPB) on each branch (PP/MPB). The *scale bar* represents the expected number of changes per site. The tree was rooted to *Seiridium* sp. (SD096)

this species was deposited in Centraalbureau voor Schimmelcultures in the Netherlands with CBS accession CBS137769.

Due to *Pestalotiopsis* group prevalence throughout the world and its broad host range, this is a potent plant pathogen that has gone largely unrecognized. The genus *Pestalotiopsis* encompasses fungi that are commonly isolated as endophytes, but also include a number of plant pathogens that cause a variety of post-harvest diseases, fruit rots and leaf spots, as well as other emerging diseases. *Pestalotiopsis* is delineated from two novel genera, namely *Neopestalotiopsis* and *Pseudopestalotiopsis*, and 35 novel

species are introduced, along with several new combinations to emend monophyly of these genera [6–9]. Therefore, distinct morphological characteristics as well as molecular data are needed to distinguish species in these genera [5].

It was already recorded that *P. longisetula*, the causal agent of strawberry fruit rot in different locations in Iran [1] and Egypt [3], could attack tomato fruits as well as three other plant species in a host range reaction to this pathogen [3]. But to our knowledge, this is the first report of *N. mesopotamica* causing fruit rot on tomato in Iran and the world. Recently, Maharachchikumbura et al. [9] introduced *N. mesopotamica* isolated from eucalyptus and pine trees as new species. The potential of Pestalotiopsis group to cause yield losses in economically important crops such as tomato, strawberry and tea warrants further study on these fungal pathogens. Since tomato industry is important in Iran, better understanding of its diseases is relevant in order to establish disease control strategies.

Acknowledgments Authors gratefully acknowledged Research Council of Bu-Ali Sina University, Hamedan, Iran, for partial financial support.

References

1. Arzanlou M, Torbati M, Khodaei S, Bakhshi M (2012) Contribution to the knowledge of pestalotioid fungi of Iran. Mycosphere 3:871–878
2. Doyle JJ, Doyle JL (1987) A rapid DNA isolation procedure for small quantities of fresh leaf tissue. Phytochem Bull 19:11–15
3. Embaby E (2007) Pestalotia fruit rot on strawberry plants in Egypt. Egypt J Phytopathol 35:99–110
4. Guba EF (1961) Monograph of Monochaeta and Pestalotia. Harvard University Press, Cambridge
5. Maharachchikumbura SSN, Guo L-D, Chukeatirote E, Bahkali AH, Hyde KD (2011) *Pestalotiopsis*—morphology, phylogeny, biochemistry and diversity. Fungal Divers 50:167–187
6. Maharachchikumbura SSN, Guo L-D, Cai L, Chukeatirote E, Wu WP, Sun X, Crous PW, Bhat DJ, McKenzie EHC, Bahkali AH, Hyde KD (2012) A multi-locus backbone tree for *Pestalotiopsis*, with a polyphasic characterization of 14 new species. Fungal Divers 56:95–129
7. Maharachchikumbura SSN, Chukeatirote E, Guo L-D, Crous PW, Mckenzie EHC, Hyde KD (2013) *Pestalotiopsis* species associated with *Camellia sinensis* (tea). Mycotaxon 123:47–61
8. Maharachchikumbura SSN, Guo L-D, Chukeatirote E, Mckenzie EHC, Hyde KD (2013) A destructive new disease of *Syzygium samarangense* in Thailand caused by the new species *Pestalotiopsis samarangensis*. Trop Plant Pathol 38:227–235
9. Maharachchikumbura SSN, Hyde K-D, Groenewald JZ, Xu J, Crous PW (2014) *Pestalotiopsis* revisited. Stud Mycol 79:121–186
10. Nylander JAA (2004) MrModeltest v2.2. Program distributed by the author: 2. Evolutionary Biology Centre, Uppsala University, Uppsala, pp 1–2
11. Ronquist F, Teslenko M, van der Mark P, Ayres DL, Darling A, Höhna S, Larget B, Liu L, Suchard MA, Huelsenbeck JP (2012) MrBayes 3.2: efficient Bayesian phylogenetic inference and model choice across a large model space. Syst Biol 61:539–542
12. Swofford DL (2003) PAUP. Phylogenetic analysis using parsimony (and other methods). Version 4. Sinauer Associates, Sunderland